Supplementary Informations for

Internalization of Antibiotics by the Multi-Resistant Bacteria Acinetobacter baumannii through the CarO Outer Membrane Porin

Florent Barbault,[*a] Antonio Monari[*a]

a) Université Paris Cité and CNRS, ITODYS F-75006 Paris, France

*florent.barbault@u-paris.fr, antonio.monari@u-paris.fr

Extended computational methodology

The initial structure of the CarO protein was retrieved from the pdb database (ID: 4RL9)[1] missing residues were reconstructed using the Swiss-Model web server,[2] while the periplasmatic unstructured tail was not considered. The protein was embedded in a lipid bilayer mimicking a realistic A. baumannii outer membrane via the help of the charmm-gui web server. The exgtracellular leaflet was constituted of specific lipopolysaccharides of the bacteria. The periplasmatic leaflet is constituted of a mixture of of 74% 1-palmitoyl-2-vacenoyl-sn-glycero-3-phosphoglycerol (PVPG), 21% 1-palmitoyl(16:0)-2-palmitoleoyl(16:1 *cis*-9)-phosphatidylethanolamine (PPPE), and 5% 1,10-palmitoyl-2,20-vacenoyl cardiolipin (PVCL2) coherently with other previous works.[3,4] A 20 Å water surface was added on top and bottom of the lipid bilayer including a 0.15 M physiological concentration of NaCl. All the MD simulations have been performed using the NAMD 3.0 code.[5,6] The protein and the lipid were represented using charmm force field while water is modeled with TIP3P.[7] The general force field of IMP was obtained from the charmm-gui server to assure compatibility with the charmm force field used troughout. Hydrogen Mass Repartion (HMR)[8] was used to allow propagating the MD simulation using a tilme step of 4 fs in combination with the Rattle and Shake algorythm.[9] All the simulations have been conducted in the isothermal and isobaric (NPT) ensemble using a Langevin thermostat and barostat[10] to maintain the temperature at 300 K and the pressure at 1 atm. Prior to production the system has been minimized to remove bad contacts, and subsequently thermalized and equilibrated by progressively removing constrins on the protein backbone during 9 million steps (36 ns). All the analysis and visualization have been carried out using VMD[11] and cpptraj.[12]

The enhanced sampling dynamics to obtain the free energy profile for the internalization of IMP has been performed using Umbrella sampling (US). To this aim a collective variable defined as the distance from the center of mass of the outer membrane polar head Phosphorous atoms (atom type PA) projected on the normal to the membrane surface has been considered. To perform the US the coordinate has been partitioned in 36 windows, a first equilibration of 50 ns has been performed for each windows followed by a production sampling extended up to 200 ns for each window. In each window the

collective varibale has been restrained with an harmonic potential of 2.5 kcal/mol by using the COLVARS module. A width of 0.1 Å was used for the binning collection. The full potential of mean force PMF has been reconstructed using the Weighted Histogram Analysis Method (WHAM).[13] The overlap between the windows and the evolution of the PMF with the sampling time have been properly checked to assure convergence. The convergence of the PMF has been carefully checked assuring the overlap between contiguous windows to ensure the consistence of the free energy reconstruction. Furthermore, the changes in the free energy have been monitored as a function of the sampling time. We may notice that the free energy change between 150 and 200 ns along the collective variable is in average of 0.2 kcal/mol and it never exceeds 0.9 kcal/mol.

References

1 M. Zahn, T. D'Agostino, E. Eren, A. Baslé, M. Ceccarelli and B. van den Berg, *J Mol Biol*, 2015, **427**, 2329–2339.

2 A. Waterhouse, M. Bertoni, S. Bienert, G. Studer, G. Tauriello, R. Gumienny, F. T. Heer, T. A. P. De Beer, C. Rempfer, L. Bordoli, R. Lepore and T. Schwede, *Nucleic Acids Res*, 2018, **46**, 296–303.

3 L. Vasseur, F. Barbault and A. Monari, *Chemistry – A European Journal*, DOI:10.1002/chem.202500874.

4 L. Vasseur, F. Barbault and A. Monari, *J Phys Chem B*, 2024, **128**, 3929–3936.

5 J. C. Phillips, R. Braun, W. Wang, J. Gumbart, E. Tajkhorshid, E. Villa, C. Chipot, R. D. Skeel, L. Kalé and K. Schulten, *J Comput Chem*, 2005, **26**, 1781–1802.

6 J. C. Phillips, D. J. Hardy, J. D. C. Maia, J. E. Stone, J. V. Ribeiro, R. C. Bernardi, R. Buch, G. Fiorin, J. Hénin, W. Jiang, R. McGreevy, M. C. R. Melo, B. K. Radak, R. D. Skeel, A. Singharoy, Y. Wang, B. Roux, A. Aksimentiev, Z. Luthey-Schulten, L. V. Kalé, K. Schulten, C. Chipot and E. Tajkhorshid, *Journal of Chemical Physics*, 2020, **153**, 044130.

7 P. Mark and L. Nilsson, *Journal of Physical Chemistry A*, 2001, **105**, 9954–9960.

8 C. W. Hopkins, S. Le Grand, R. C. Walker and A. E. Roitberg, *J Chem Theory Comput*, 2015, **11**, 1864–1874.

9 S. Miyamoto and P. A. Kollman, *J Comput Chem*, 1992, **13**, 952–962.

10 R. L. Davidchack, R. Handel and M. V. Tretyakov, *Journal of Chemical Physics*, 2009, **130**, 234101.

11 W. Humphrey, A. Dalke and K. Schulten, *J Mol Graph*, 1996, **14**, 33–38.

12 V. V. Shitov, N. A. Semenov and N. Y. Gozman, *Telecommunications and Radio Engineering (English translation of Elektrosvyaz and Radiotekhnika)*, 1984, **38–39**, 14–16.

13 A. Grossfield, *Analysis*, 2004, 1–13.

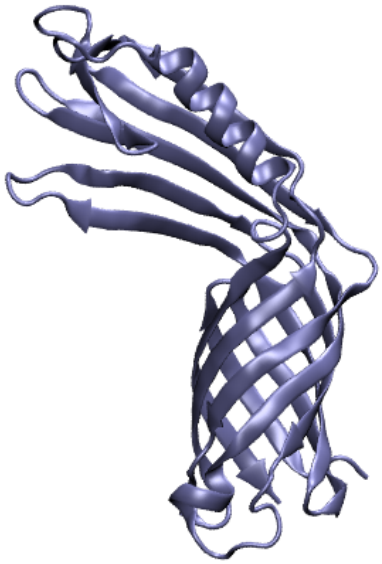

Figure S1. Initial structure of the CarO protein has extracted from the pdb database (4RL9)

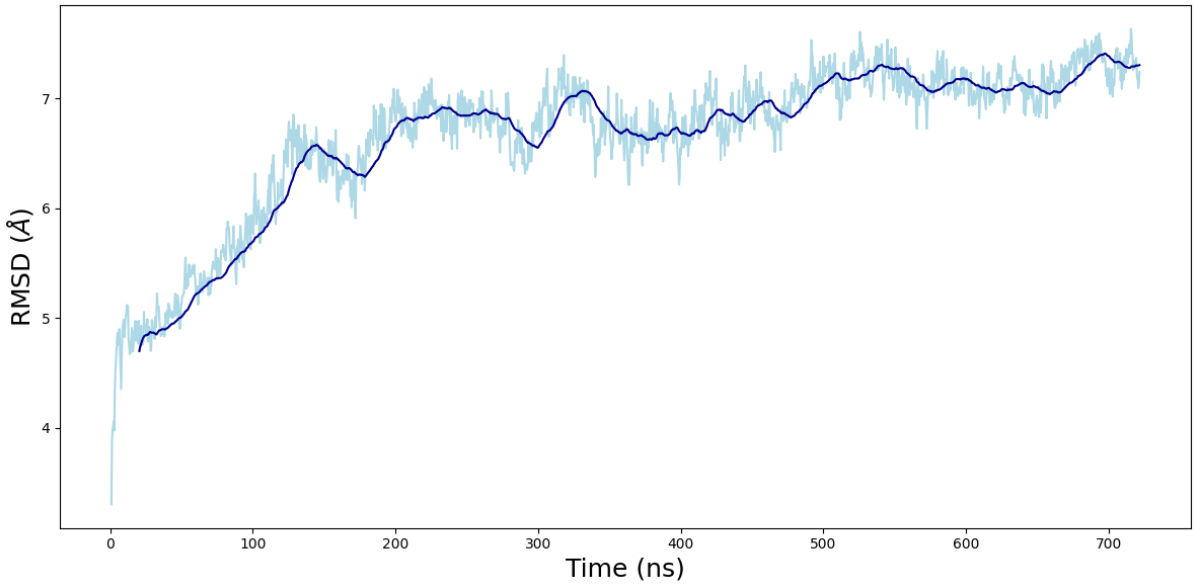

Figure S2. Time evolution of the RMSD for the CarO protein embedded in the lipid bilayer during the equilibrium MD.

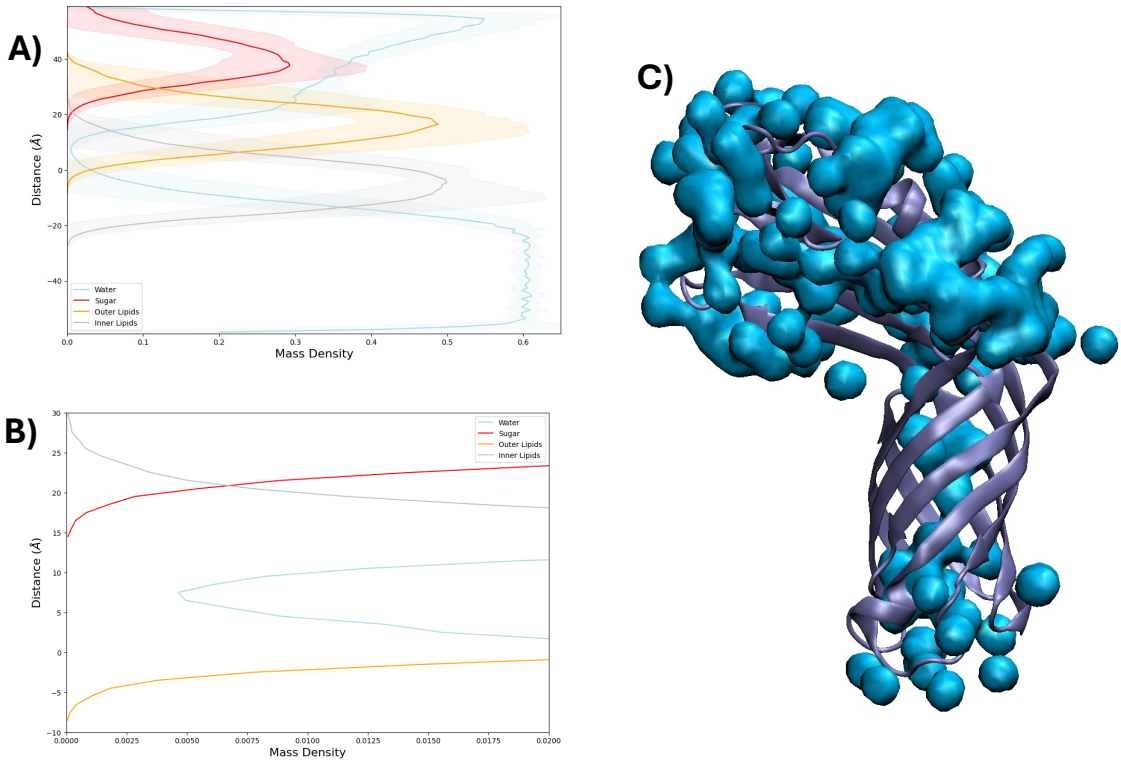

Figure S3. A) Density profile along the normal to the lipid bilayer plane for the different components of the membrane system, i.e. water, sugar, and extracellular and periplasmatic lipids. B) A zoom focusing on the center of the membrane showing the non-zero density of water due to the presence of the CarO porin. C) A representative snapshot from the MD simulation showing formation of a water channel through the protein.

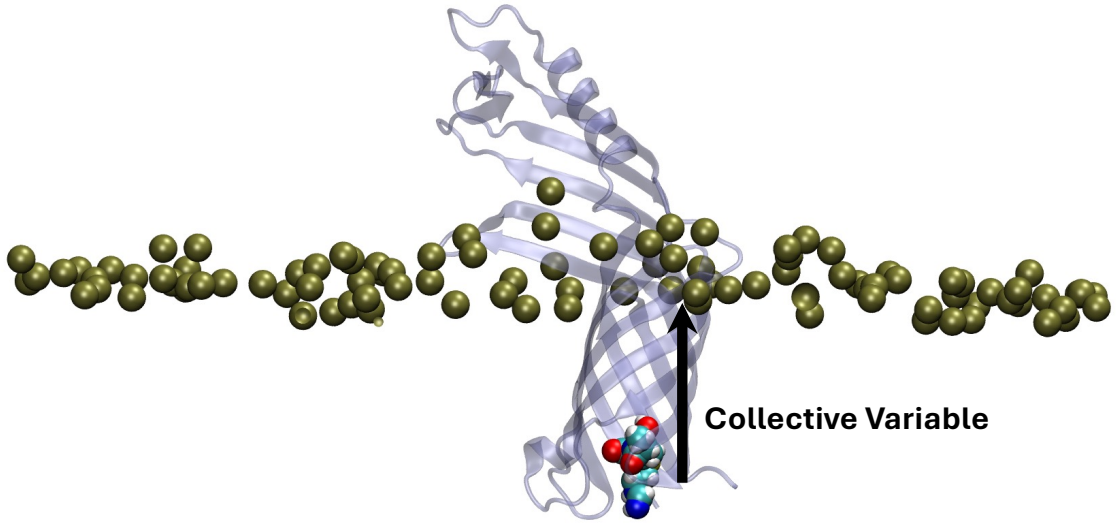

Figure S4. Pictorial representation of the Collective Variable used for the Umbrella Sampling procedure.

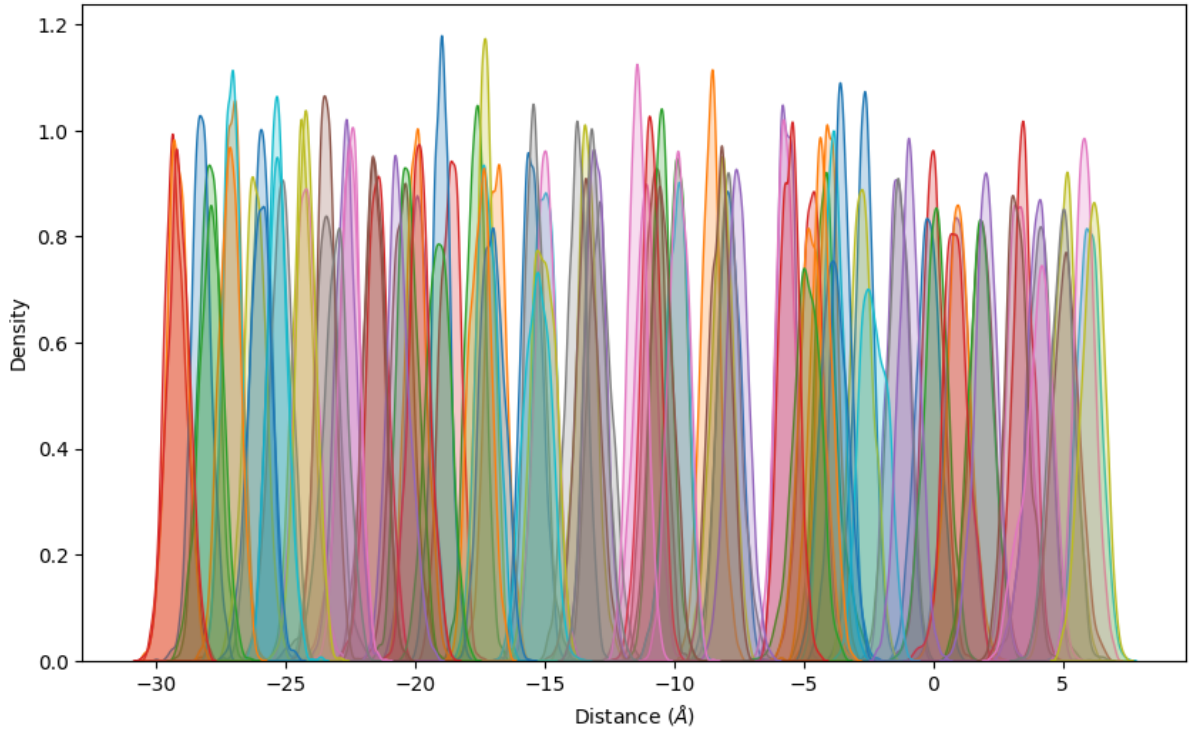

Figure S5. Distribution of the collective variable values over the different windows showing the consistent overlap.

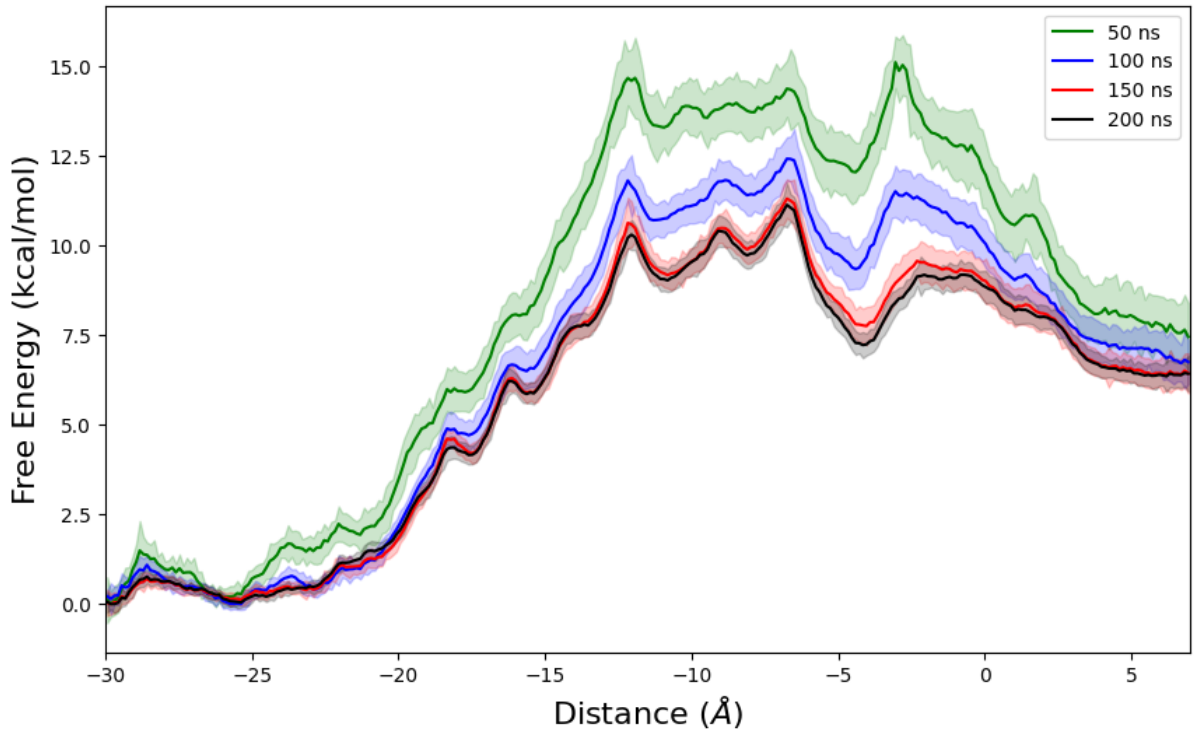

Figure S6. Convergence of the PMF profile with the sampling time.